ASSESSMENT OF THE INDOOR AIR PURIFICATION BY PHOTOCATALYTIC PAINTS

F. SALVADORES, O.M. ALFANO and M.M. BALLARI

† *INTEC (Universidad Nacional del Litoral – CONICET), Santa Fe, Argentina.*
alfano@intec.unl.edu.ar

***Abstract*— Photocatalytic building materials containing TiO_2 were extensively studied for outdoor applications using solar radiation. Nowadays, the market offers a wide variety of these materials with self-cleaning and air purification functionalities. However, heterogeneous photocatalysis applied in indoor construction materials was less developed. The objective of this work is to investigate the photocatalytic performance of carbon doped TiO_2 in replacement of the normal pigments in indoor wall paint formulations. To achieve this goal, the photocatalytic oxidation of acetaldehyde in gas phase was carried out. The air decontamination process was conducted using regular indoor light in a bench scale chamber photoreactor simulating a room. The main environmental conditions that affect the photocatalytic process were varied: air flow rate, irradiance, relative humidity and acetaldehyde concentration. The results were analyzed through the response surface methodology and revealed the air purifying power of photocatalytic paints under indoor conditions.**

***Keywords*— Photocatalysis; Paint; Indoor; Air; Depollution.**

I. INTRODUCTION

Several chemical air pollutants are continually emitted to indoor environments affecting the wellness and health of people. These air contaminants can cause drowsiness, headache, sore throat, mental fatigue, allergies, asthma, eyes, nose and throat irritation, and dizziness, among others health problems. One of the problematic Volatile Organic Compounds (VOCs) in indoor and outdoor environments is the acetaldehyde. This pollutant is toxic, irritant and probable carcinogen, and it can be released by burning processes and building materials in homes.

The heterogeneous photocatalysis has proven to be an efficient method for the chemical and biological purification of water and air. The most studied photocatalyst is titanium dioxide (TiO_2) that can be activated by UV radiation (200-400 nm), which is scanty in indoor lighting and only about 4% of the total solar radiation. To extend the radiation absorption of TiO_2 to wavelengths corresponding to the visible spectrum (400-700 nm), several modification methods like dye sensitization and doping with transition metals or with nonmetals were developed (Banerjee *et al*., 2014; Wang *et al*., 2014).

The use of TiO_2 to develop photocatalytic materials that can be applied on building structures is becoming an alternative technology for the degradation of air pollutants (Ballari and Brouwers, 2013; Faraldos *et al*., 2015; Tang *et al*., 2019).

One of the most employed materials in construction is the wall paint or coating with aesthetic and protecting functions. Several studies were focused on the application of photocatalytic TiO_2 in different indoor and outdoor paint formulations. These works have analyzed: i) the air decontamination capability employing several model pollutants (Aguia *et al*., 2011; Gandolfo *et al*., 2015; Monteiro *et al*., 2015); ii) colorant bleaching over the irradiated paint to assess self-cleaning properties (Hochmannova and Vytrasova, 2010); and iii) inactivation of bacteria and fungi (Zuccheri *et al*., 2013, Zacarías *et al*., 2018). However, in most of these studies, UV radiation was tested as the energy source to activate the paints and lab scale photoreactors were employed to carry out the experiments.

In the present work, the degradation of acetaldehyde in air was carried out employing photocatalytic wall paints and normal indoor illumination in a bench scale chamber photoreactor that simulates the ambient conditions of a room.

II. METHODS

A. Photocatalytic paint formulation

A carbon doped TiO_2 powder KRONOClean 7000 was employed to formulate the photocatalytic paint in replacement of the normal paint pigments. The formulated photocatalytic paint is composed by water (30% w/w), styrene-acrylic resin (33% w/w), $CaCO_3$ (18% w/w), TiO_2 (18% w/w), and dispersing agent (1% w/w).

The paint application was made with an aerograph on paper sheets with a total area of 5100 cm^2 to cover the walls of the bench scale chamber photoreactor. Due to the difficulty of deposit the exact same quantity of paint in the walls reactor, the side walls were coated with $(7.7\pm1.2)\times10^{-4}$ g cm^{-2} of dry paint and the front walls with $(4.5\pm1.2)\times10^{-4}$ g cm^{-2}.

The prepared coatings were dried at 25ºC for 24 hours. Previously to the decontamination tests, the photocatalytic samples were cured exposing them under visible light for a period of time between 5 and 8 hours. With this procedure, the paint organic compounds that surround the photocatalytic particle were oxidized, allowing latter the interaction between the air contaminant and the TiO_2 present in the paint.

The photocatalytic coating was characterized by measurements of the optical properties and microscopic images. The paint was deposited with the methodology described above on both sides of acrylic plates and, after the samples were dried, the diffuse reflectance ($R_{p,a,p}$) and

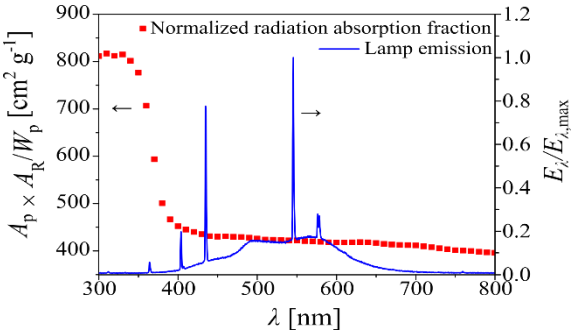

Fig. 1: Indoor lamp spectral emission and fraction of absorbed radiation by the photocatalytic paint

diffuse transmittance ($T_{p,a,p}$) were measured in a spectro-radiometer Optronic OL Series 750 with integrating sphere. Performing a radiation flux balance in the three layers system (paint-acrylic-paint), the absorption radiation fraction of the paint layer (A_p) can be calculated as follows (Ballari *et al.*, 2016):

$$A_{p,\lambda} = 1\text{-}R_{p,\lambda}\text{-}T_{p,\lambda} \quad (1)$$

where:

$$R_{p,\lambda} = \frac{R_{p,a,p,\lambda}\,T_{a,\lambda}\text{-}T_{p,a,p,\lambda}\,R_{a,\lambda}}{T_{p,a,p,\lambda}\,T_{a,\lambda}^2\text{-}T_{p,a,p,\lambda}\,R_{a,\lambda}^2+T_{a,\lambda}} \quad (2)$$

$$T_{p,\lambda} = \sqrt{\frac{\left(R_{p,a,p,\lambda}\text{-}R_{p,\lambda}\right)\left[1\text{-}R_{p,\lambda}\left(R_{acr,\lambda}+\dfrac{T_{a,\lambda}^2 R_{p,\lambda}}{1\text{-}R_{a,\lambda}R_{p,\lambda}}\right)\right]}{R_{a,\lambda}+\dfrac{T_{a,\lambda}^2 R_{p,\lambda}}{1\text{-}R_{a,\lambda}R_{p,\lambda}}}} \quad (3)$$

where R_a and T_a are the experimental diffuse reflectance and transmittance, respectively, of the acrylic support.

The spectral absorption radiation fraction per unit of weight of deposited paint and unit of superficial area is shown in Fig. 1. It can be seen that the paint presents a high absorption radiation fraction for values lower than 350 nm (ultraviolet radiation), after which it decreases and remains almost constant for the visible range (>400 nm). Also, the prepared samples were observed in a Scanning Electron Microscope (SEM) JEOL JSM-35C. The side view of the photocatalytic coating is shown in Fig. 2, presenting a homogeneous thickness of approximately 11 μm.

B. Photocatalytic reactor and experimental procedure

The experimental setup to carry out the photocatalytic degradation of acetaldehyde in gas phase is shown in Fig. 3. It consists of a bench scale chamber photoreactor with a fan inside to ensure good mixing conditions and whose walls were covered by paper coated with the photocatalytic paint. The photocatalytic reactor was irradiated with fluorescent visible light lamps on the top and fed by certificated PRAXAIR acetaldehyde gas stabilized in nitrogen (300 ppm), mixed with air to reach the chosen inlet pollutant concentration. The spectral emission of the lamps is shown in Fig. 1. The outlet and inlet contaminant concentrations from the reactors were analyzed employing gas chromatography with a flame ionization detector (FID), performing a direct injection of the gas sample.

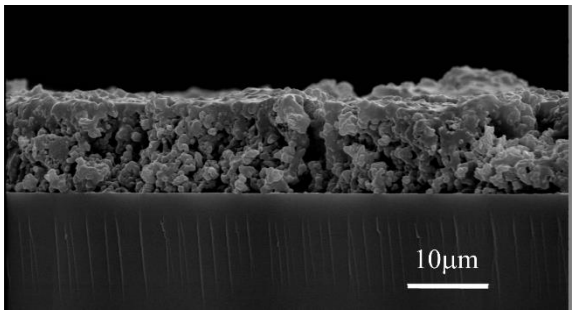

Fig. 2: SEM side view of the photocatalytic paint coating.

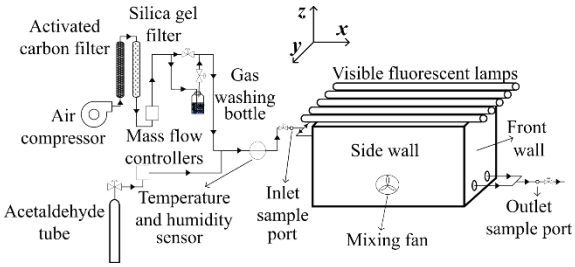

Fig. 3: Experimental setup to carry out acetaldehyde photocatalytic degradation

The radiation flux on the front and side reactor walls was measured with an ILT 1700 radiometer with a SED033/F/W visible light sensor (400 – 1064 nm) (Fig. 4). Table 1 shows the main characteristics, dimensions and operating conditions of the experimental setup to carry out the acetaldehyde photocatalytic degradation experiments.

C. Experimental design and Response Surface Methodology (RSM)

To simulate a normal room environment, the operating conditions of the bench scale photoreactor were changed according to a D-optimal experimental design selecting three numerical factors (irradiation level, flow rate and relative humidity) varied in three levels, and one categorical factor (inlet acetaldehyde concentration) varied in two levels. Regarding the variation of the flow rate, air change rates of 0, 2.85 and 5.7 times per hour were selected to simulate different ventilation conditions of a room. In Fig. 5, the resulting 22 different air depolluting experiments are schematized. The analysis of the experimental data was done with the Response Surface Methodology (RSM) applying a reduced quadratic model with a logit transformation of the response, the acetaldehyde conversion X_{Acet} [%] and the global conversion X_{Global} [%] taking into account the formaldehyde formation as a reaction intermediate:

$$\ln\frac{X}{100-X} = a + bH + cQ + dR + eC_{Acet,in} + fH^2 + gQ^2 + hR^2 \quad (4)$$

where H is the relative humidity, Q the air flow rate, R the radiation level, $C_{Acet,in}$ the inlet concentration of acetaldehyde, a to h are the coefficients of the model to be estimated, and X is the acetaldehyde or global conversion, defined as:

$$X_{Acet} = \frac{C_{Acet,in} - C_{Acet,out}}{C_{Acet,in}} \times 100 \quad (5)$$

Table 1: Bench scale chamber photoreactor characteristics and operating conditions.

Reactor volume, V_R	52500 cm^3
Residence time	630 s (for the maximum flow rate)
Visible light lamps	5 × OSRAM EVERSUN L40/79K 40 W, on the top of the photoreactor
Average paint specific load, W_p/A_R	(6.1±2.3)×10^{-4} g cm^{-2}
Total photocatalytic surface area, A_R	5100 cm^2
Air flow rate, Q	0-5000 cm^3 min^{-1}
Relative humidity, H	28-75%
Incident radiation flux, q_w / Radiation level, R	7.8 - 34.9 W m^{-2} / 22.3 - 100%
Inlet pollutant concentration, $C_{Acet,in}$	2.5 - 5 ppm

$$X_{Global} = \frac{C_{Acet,in} - C_{Acet,out} - C_{Form,out}}{C_{Acet,in}} \times 100 \qquad (6)$$

where $C_{Acet,out}$ and $C_{Form,out}$ are the chamber outlet concentrations of acetaldehyde and formaldehyde, respectively. These concentrations correspond to the steady state for continuous flow experiments, while for the batch mode C_{out} at 200 min after the photocatalytic reaction started was chosen.

The selected factors significance on the acetaldehyde and global conversions was analyzed through an Analysis of Variance (ANOVA).

D. Experiments outside the experimental design

Three additional experiments were done to compare the reaction and efficiencies of the photocatalytic process with respect to the location of the reactor walls. All these experiments were carried out at $C_{Acet,in}$=5ppm, H=50%, Q =2500 cm^3 min^{-1} and R=100%. The first one was done with all the walls covered with photocatalytic paint (A_R=5100 cm^2), the second with only the side walls painted (A_R=3000 cm^2) and the last one in which the front walls were the only photocatalytically active surfaces (A_R=2100 cm^2).

To compare the photocatalytic performance of the three configurations, the photonic and quantum efficiencies were computed according to Eqs. (7) and (8), respectively. These efficiencies relate the contaminant reaction rate with the incident radiation flux on the photocatalytic wall (photonic efficiency, $\eta_{p,Acet}$) and with the radiation absorbed by the photocatalytic paint (quantum efficiency, $\eta_{q,Acet}$).

$$\eta_{p,Acet} = \frac{\langle r_{Acet} \rangle}{\left\langle \sum_{\lambda} q_{w,\lambda} \right\rangle} \qquad (7)$$

$$\eta_{q,Acet} = \frac{\langle r_{Acet} \rangle}{\left\langle \sum_{\lambda} e^{a}_{s,\lambda} \right\rangle} = \frac{\langle r_{Acet} \rangle}{\left\langle \sum_{\lambda} q_{w,\lambda} A_{p,\lambda} \right\rangle} \qquad (8)$$

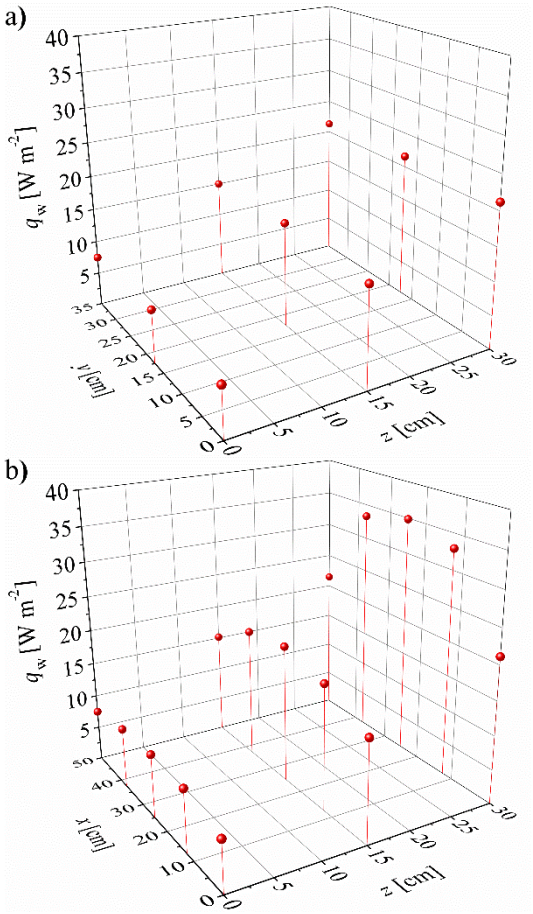

Fig. 4: Measured radiation flux on a) front walls and b) side walls

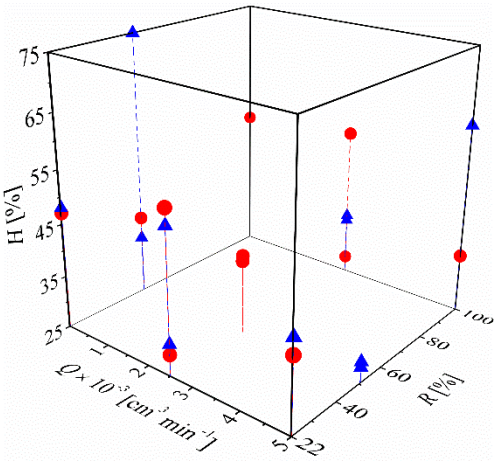

Fig. 5: D-Optimal experimental design. ● $C_{Acet,in}$=2.5 ppm, ▲ $C_{Acet,in}$=5 ppm

where r_{Acet} is the acetaldehyde reaction rate, $q_{w,\lambda}$ the spectral incident radiation flux, $A_{p,\lambda}$ the spectral radiation absorption fraction by the paint, and $e^{a}_{s,\lambda}$ the Local Superficial Rate of Photons Absorption (LSRPA).

To account for the average acetaldehyde reaction rate, Eq. (9) was used:

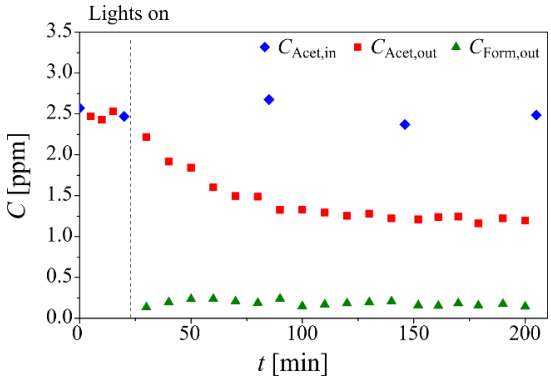

Fig. 6: Typical experimental run (H=28%, Q=2500 cm^3 min^{-1}, R=100% and $C_{Acet,in}$=2.5ppm)

$$\langle r_{Acet} \rangle = \frac{Q\left(C_{Acet,in} - C_{Acet,out}\right)}{A_R} \quad (9)$$

where Q is the air flow rate and A_R is the photocatalytic surface area.

Also, the decrease of acetaldehyde concentration by means of mechanical ventilation alone was compared with ventilation plus photocatalytic oxidation. To do this, once the pollutant concentration reached 5 ppm in the reactor, the acetaldehyde inlet was closed and the gas flow contained only unpolluted air at 2500 cm^3 min^{-1}. This was done with and without the presence of photocatalytic walls.

III. RESULTS AND DISCUSSION

E. Acetaldehyde photocatalytic degradation

Figure 6 presents a typical experimental run of photocatalytic oxidation of acetaldehyde. When the lights are turned on, the acetaldehyde concentration diminishes while the formaldehyde, a reaction intermediate, is produced and then its concentration remains almost constant. This is in concordance with the photocatalytic oxidation mechanism of acetaldehyde, which is degraded first to formaldehyde, then to formic acid, to finally be converted in CO_2 through the attack of hydroxyl radical formed during the hole trapping of the photocatalyst (Salvadores *et al.*, 2016). However, for the reaction conditions and analytical method employed in this work, no formic acid was detected and low formaldehyde concentration was produced. By varying the different operating conditions within the experimental design, acetaldehyde conversions changed between 6 and 92% while the global conversion varied between 3 and 71%.

After several experiments totaling more than 140 hours of reaction time with the same paint coating, no photocatalyst deactivation was observed. Apart from that, in previous tests, acetaldehyde was not photodegraded on a non-photocatalytic paint formulated with rutile instead of anatase TiO_2.

F. Influence of environmental conditions

In Fig. 7, the acetaldehyde conversion is shown by varying the inlet acetaldehyde concentration, the relative humidity and the irradiance level operating in batch mode (Fig. 7a) and continuous mode (Figs. 7b and c), according to the D-Optimal experimental design.

An inverse relationship between relative humidity and air flow rate with the conversion was observed, i.e. the lower the humidity and the air flow rate, the higher the conversion. For lower air flow rate, the residence time of the acetaldehyde in the reactor is increased. On the other hand, the water vapor molecules are adsorbed onto the active sites of the photocatalyst. So, if the humidity is low, less water molecules compete with the acetaldehyde and the reaction rate is increased. As expected, for higher radiation level an increase of conversion was observed because of an increase in the photocatalyst activation rate. In addition, the acetaldehyde conversion was not influenced by the inlet pollutant concentration, indicating an almost pseudo first order reaction rate.

The coefficients of the response surfaces for acetaldehyde and global conversions (Eq. 4) were fitted with the experimental data and are shown in Table 2. The coefficient of determination of the model is c.a. 0.93 for acetaldehyde and global conversions, showing that the surfaces are in good agreement with the experimentally determined conversions.

The surface corresponding to acetaldehyde conversion is shown in Fig. 7, while the surface for the global conversion presented a similar behavior (results not shown).

An ANOVA was carried out to statistically verify the significance of the varied factors on the selected response (Table 2). When the p-value is less than 0.05, the effect is considered significant. So, the significant effects for the acetaldehyde and global conversions were the linear and quadratic terms of the irradiance level, relative humidity and flow rate factors. Conversely, the p-values corresponding to the inlet acetaldehyde concentration are greater than 0.1, indicating that is a non-significant factor

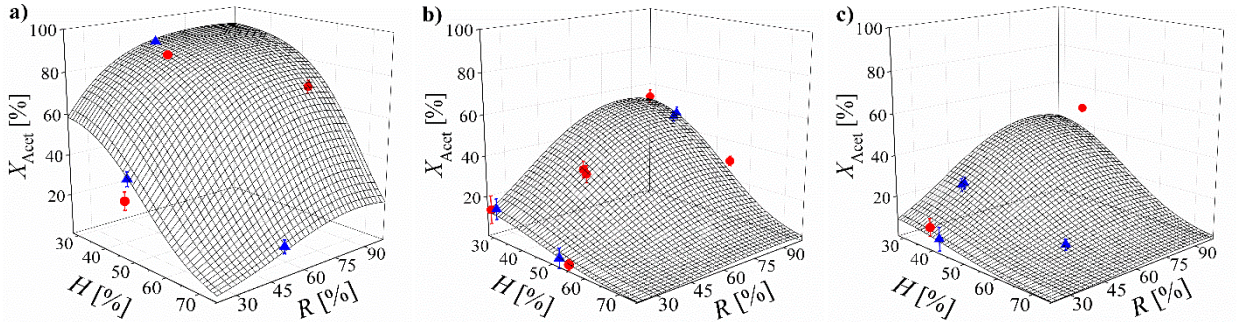

Fig.7: Surface response and experimental data for acetaldehyde conversion. a) Q=0 cm^3 min^{-1}, t=200 min. b) Q=2500 cm^3 min^{-1}, steady state. c) Q=5000 cm^3 min^{-1}, steady state. ● $C_{Acet,in}$=2.5 ppm, ▲ $C_{Acet,in}$=5 ppm

Table 2: ANOVA and surface response for acetaldehyde and global conversions

		X_{Acet}		X_{Global}	
Model factor	Coefficient	Estimated value	p- value	Estimated value	p- value
Intercept	a	-2.5224		-3.7176	
H	b	0.0868	< 0.0001	0.0871	< 0.0001
Q	c	-1.2982	< 0.0001	-1.0002	< 0.0001
R	d	0.0890	< 0.0001	0.0827	< 0.0001
$C_{Acet,in}$	e	-0.0009	0.9921	0.0981	0.2322
H^2	f	-0.0016	0.0234	-0.0015	0.0203
Q^2	g	0.1519	0.0009	0.1051	0.0076
R^2	h	-0.0005	0.0096	-0.0004	0.0113
Coefficient of determination		0.9297		0.9313	

Table 3: Parameters for analysis of reactor walls locations

	Photoreactor walls		
	All	Front	Side
$A_R \times 10^1$ [m^2]	5.1	2.1	3.0
X_{Acet} [%]	44.6	12.3	33.7
$\left\langle \sum_{\lambda} q_{w,\lambda} \right\rangle \left[\mathrm{W\,m^{-2}} \right]$	15.3	14.1	16.5
$\left\langle \sum_{\lambda} e^{a}_{s,\lambda} \right\rangle \times 10^6 \left[\mathrm{Einstein\,m^{-2}\,s^{-1}} \right]$	9.7	6.5	12.9
$\langle r_{Acet} \rangle \times 10^9 \left[\mathrm{mol\,m^{-2}\,s^{-1}} \right]$	7.46	4.98	9.48
$\eta_{p,Acet} \times 10^5$	10.5	7.61	12.4
$\eta_{q,Acet} \times 10^4$	7.69	7.66	7.35

for both conversions and confirming a pseudo-first order kinetics.

G. Relative positions of the photocatalytic surfaces

In Table 3 several results are shown for the experiments changing the photocatalytic surfaces location with respect to the lamps positions (walls in front and back to the lamps, or walls on both sides of the lamps). First, the acetaldehyde conversion increases with the photocatalytic surface area (A_R), but not in the same proportion. It can be also observed that the average incident radiation flux is slightly higher for the lateral walls parallel to the lamps (see also Fig. 4). In the side walls the radiation comes from the whole length of the lamp, while the front walls mainly receive radiation from the end of the lamp. Note that the LSRPA corresponding to side walls is almost twice than for the front walls. This is also due to deviations from the deposited paint load on the different reactor walls. On the other hand, the $\langle r_{Acet} \rangle$ is also almost twice for the side walls comparing to front walls due to the relative location of the surface regarding the lamps but also to the differences in photocatalytic coating amounts. So, to compare the different situations, the photonic and quantum efficiencies can be evaluated. The side walls present the highest photonic efficiency value because the superficial reaction rate increases more than the incident radiation flux in the denominator of Eq. (7) due to a higher deposited paint amount. In contrast, quantum efficiencies became similar for the three experiments independently of surface location. This is due to the fact that in all the walls the numerator and denominator of Eq. (8) are proportional because both vary with the incident radiation flux and catalyst amount.

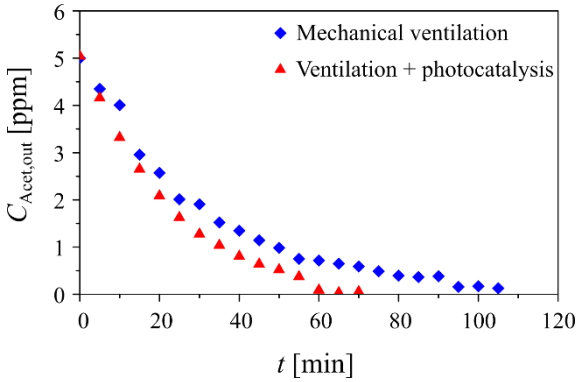

Fig. 8: Comparison of acetaldehyde decontamination applying mechanical ventilation alone and with photocatalytic paint in the walls (H=50%, Q=2500 cm^3 min^{-1}, R=100%).

H. Comparison of two different air decontamination processes

Figure 8 shows the comparison of the decrease in acetaldehyde concentration applying two different decontamination processes: (i) mechanical ventilation alone and (ii) mechanical ventilation combined with photocatalysis. The time to achieve an acetaldehyde concentration reduction of 95% was around 90 min for the mechanical ventilation alone, while it was 55 min for the combined process (about 40% faster). This is also in concordance with the calculated initial acetaldehyde removal rate, being this for the photocatalytic system about 38% higher than that of the ventilation one.

IV. CONCLUSIONS

The scaling up of air depolluting experiments was carried out using a photocatalytic wall paint in a bench scale chamber photoreactor. A D-optimal experimental design was applied, and acetaldehyde and global conversions were satisfactorily fitted with the Surface Response Methodology (RSM) applying a reduced quadratic model with a logit transformation of the response.

According to the ANOVA, the relative humidity, the radiation level and the air flow are significant factors for the applied model for the acetaldehyde and global conversions. In contrast, the acetaldehyde conversion was not influenced by the inlet pollutant concentration.

Also, other experiments were done outside the experimental design. In the first set, the location of the photocatalytic surface regarding the lamps was evaluated. It was determined that for an optimal air purification in terms of the pollutant conversion, the photocatalytic surfaces should be parallel to the lamp axis. In another set of experiments, two methods for the pollutant reduction in the bench scale chamber photoreactor was compared, being the mechanical ventilation combined with photocatalysis almost 40% faster than the mechanical removal alone.

The achieved results in the present work are useful for future implementation of photocatalytic paints in real indoor environments.

AKNOWLEDGEMENTS

The authors are grateful to Universidad Nacional del Litoral (UNL), Consejo Nacional de Investigaciones Científicas y Técnicas (CONICET), and Agencia Nacional de Promoción Científica y Tecnológica (ANPCyT) of Argentina for financial support. Eugenia Barros, Graciana Bertoni and Guillermina Díaz are acknowledged for their help in experimental work. Kronos is thanked for the provided photocatalyst. BASF Argentina is thanked for the provided resin and dispersant agent.

REFERENCES

Águia, C., Ângelo, J., Madeira, L.M. and Mendes, A. (2011) "Influence of paint components on photoactivity of P25 titania toward no abatement" *Polym. Degrad. Stab.*, **96**, 898–906.

Ballari, M.M. and Brouwers, H.J.H. (2013) "Full scale demonstration of air-purifying pavement" *J. Hazard. Mater.*, **254-255**, 406–414.

Ballari, M.M., Carballada, J., Minen, R.I., Salvadores, F., Brouwers, H.J.H., Alfano, O.M. and Cassano, A.E. (2016) "Visible Light TiO_2 Photocatalysts Assessment for Air Decontamination" *Process Saf. Environ. Prot.*, **101**, 124–133.

Banerjee, S., Pillai, S., Falaras, P., O'Shea, K.E., Byrne, J.A. and Dionysiou, D.D. (2014) "New insights into the mechanism of visible light photocatalysis" *J. Phys. Chem. Lett.*, **5**, 2543–2554.

Faraldos M., Kropp, R., Anderson, M.A. and Sobolev, K. (2015) "Photocatalytic hydrophobic concrete coatings to combat air pollution" *Catal. Today*, **258**, 228–236.

Gandolfo, A., Bartolomei, V., Gomez Alvarez, E., Tlili, S., Gligorovski, S., Kleffmann, J. and Wortham, H. (2015) "The effectiveness of indoor photocatalytic paints on NOx and HONO levels" *Appl. Catal. B*, **166-167**, 84–90.

Hochmannova, L. and Vytrasova, J. (2010) "Photocatalytic and antimicrobial effects of interior paints" *Prog. Org. Coat*., **67**, 1-5.

Monteiro, R.A.R., Silva, A.M.T., Ângelo, J.R.M., Silva, G.V., Mendes, A.M., Boaventura, R.A.R. and Vilar, Vítor, J.P. (2015) "Photocatalytic oxidation of gaseous perchloroethylene over TiO_2 based paint" *J. Photochem. Photobiol. A*, **311**, 41–52.

Salvadores, F., Minen, R.I., Carballada, J., Alfano, O. M. and Ballari, M.M. (2016) "Kinetic study of acetaldehyde degradation applying visible light photocatalysis" *Chem. Eng. Technol.*, **39**, 166–174.

Tang, X., Ughetta, L., Shannon, S.K., Houzé de l'Aulnoita, S., Chen, S., Gould, R.A.T., Russell, M.L., Zhang, J., Ban-Weiss, G., Everman, R.L.A., Klink, F.W., Levinson, R. and Destaillats, H. (2019) "De-pollution efficacy of photocatalytic roofing granules" *Build. Environ.*, **160**, 106058.

Wang, Z., Liu, Y., Huang, B., Dai, Y., Lou, Z., Wang, G., Zhang X. and Qin, X. (2014) "Progress on extending the light absorption spectra of photocatalysts" *Phys. Chem. Chem. Phys.*, **16**, 2758.

Zacarías, S.M., Marchetti, S., Alfano, O.M. and Ballari M.M. (2018) "Photocatalytic paint for fungi growth control under different environmental conditions and irradiation sources" *J. Photochem. Photobiol. A*, **364**, 76–87.

Zuccheri, T., Colonna, M., Stefanini, I., Santini, C. and Di Gioia, D. (2013) "Bactericidal activity of aqueous acrylic paint dispersion for wooden substrates based on TiO_2 nanoparticles activated by fluorescent light" *Mater.*, **6**, 3270-3283.

Received October 21, 2019
Sent to Subject Editor October 21, 2019
Accepted December 9, 2019
Recommended by Guest Editor: Carlos Apesteguia